Article

Discovery Medicine 2026; 38(206): 739–752
https://doi.org/10.24976/Discov.Med.202638206.61

Protective Mechanisms of Tight Junction Proteins in Acute Kidney Injury: A Study on the Dual Regulation of Inflammation and Oxidative Stress

Yichao Zhang[1], Huafen Shen[1], Jianrong Wu[1], Ting Liu[1], Pinqiong Qin[1], Weiqun Zhang[1,*]

[1]Department of Clinical Laboratory, The First People's Hospital of Lin'an District, 311399 Hangzhou, Zhejiang, China
*Correspondence: 13588232311@163.com (Weiqun Zhang)
Submitted: 25 November 2025 Revised: 30 January 2026 Accepted: 10 February 2026 Published: 20 March 2026

Background: Acute kidney injury (AKI) is clinically characterized by a rapid deterioration of renal function and is often associated with inflammation and oxidative stress. This study elucidated protective roles and underlying mechanisms of tight junction (TJ) proteins in AKI, with particular emphasis on the involvement of the TYRO protein tyrosine kinase binding protein (TYROBP) (also known as DNAX-associated protein 12 [DAP12])/phosphoinositide 3-kinase (PI3K)/protein kinase B (AKT) signaling pathway.

Methods: After establishing a cisplatin-induced AKI model, TJ protein levels, inflammation and oxidative stress were evaluated. ZO-1 (TJP1)-related genes were identified using Weighted Gene Co-Expression Network Analysis (WGCNA) and Protein-Protein Interaction (PPI) network analysis. An HK-2 cell injury model was established using cisplatin, followed by assessment of the impact of DAP12 silencing on TJ proteins, inflammation, oxidative stress, and PI3K/AKT signaling pathway. Renal function, inflammation (tumor necrosis factor-α [TNF-α] and interleukin-1β [IL-1β]), oxidative stress (reactive oxygen species [ROS] and malondialdehyde [MDA]), and TJ protein levels were determined through histopathology, Western blotting and enzyme-linked immunosorbent assay (ELISA).

Results: Cisplatin-induced AKI resulted in downregulated TJ proteins (ZO-1, Occludin, Claudin-1), elevated inflammation and oxidative stress, and activated DAP12/PI3K/AKT ($p < 0.05$). Among the three TJ proteins, only TJP1 level was diminished in kidney injury-related diseases. Then, through WGCNA and PPI analysis, DAP12 was identified as a key gene negatively correlated with TJP1. DAP12 silencing in the HK-2 cell injury model attenuated cellular damage, restored TJ protein expression, and reduced inflammation and oxidative stress, concomitantly suppressing the activation of the PI3K/AKT pathway ($p < 0.01$).

Conclusion: Targeting the DAP12/PI3K/AKT pathway and TJ proteins presents therapeutic potential for AKI, and the upstream and downstream mechanisms of DAP12 in kidney injury warrant further investigation.

Keywords: acute kidney injury; tight junctions; inflammation; oxidative stress

Introduction

Acute kidney injury (AKI) is a prevalent clinical syndrome primarily characterized by a sudden decline in renal function [1], resulting in the accumulation of metabolic waste and toxins in the body, as well as disruptions in water-electrolyte and acid-base homeostasis [2,3]. The onset and progression of AKI involve multiple complex pathophysiological processes, among which inflammation and oxidative stress are considered pivotal mechanisms [4,5]. Of note, these two processes are interrelated and mutually reinforcing. Specifically, inflammatory cell infiltration and release of inflammatory mediators can exacerbate oxidative stress, while oxidative stress can further activate relevant signaling pathways and promote the release of inflammatory mediators, thereby forming a detrimental cycle [6–8]. Therefore, effectively reducing inflammatory responses and oxidative stress levels is of great significance for protecting the kidneys from damage and promoting the recovery of renal function, which may be a promising therapeutic avenue for AKI.

Tight junctions (TJs), as important connection structures between renal tubular epithelial cells, are mainly composed of claudin family proteins, junctional adhesion molecules (JAMs), Occludin, and zonula occludens proteins (ZO-1, ZO-2, ZO-3) [9]. Their integrity and functional stability are essential for renal protection and physiological function [10]. Recent studies have shown that TJ proteins are aberrantly expressed in various kidney diseases and are closely related to disease progression and prognosis [11,12]. TJ protein dysregulation is a common feature in various forms of AKI [13]. In cisplatin-induced nephrotoxicity models, this dysregulation manifests as a significant reduction in TJ protein expression [14], suggesting their potential involvement in disease pathogenesis. However, the specific mechanisms underlying the aberrant expression of

TJ proteins and their potential interaction with inflammation and oxidative stress responses in AKI warrant further elucidation.

This study was designed to further investigate the protective roles and underlying mechanisms of TJ proteins in AKI. We identified multiple genes associated with ZO-1 (also known as TJP1) through Weighted Gene Co-Expression Network Analysis (WGCNA) and Protein-Protein Interaction (PPI) network analysis, and found that TYRO protein tyrosine kinase binding protein (TYROBP, also termed DNAX-associated protein 12 [DAP12]) is a key negatively correlated gene. Reportedly, DAP12 is a new candidate gene associated with renal ischemia-reperfusion injury, and is highly expressed in hypoxic human kidney (HK-2) cells [15]. Moreover, DAP12 is a macrophage M1-related Hub gene shared by AKI and acute rejection (AR) after kidney transplantation, suggesting its diagnostic utility [16]. FcγRIIb aggravates lipopolysaccharide (LPS)-induced neuroinflammation via binding with DAP12 and activating phosphoinositide 3-kinase (PI3K)/protein kinase B (AKT) signaling pathway in microglia [17]. In rheumatoid arthritis, phosphorylation of the tyrosine residue within the immunoreceptor tyrosine-based activating motif (ITAM) of DAP12 induces recruitment of Syk tyrosine kinase, ultimately activating the PI3K and extracellular signal-regulated kinase (ERK) signaling pathways [18]. Furthermore, butyrate has been shown to upregulate the expression of ZO-1, Occludin, and E-cadherin in HK-2 cells by inhibiting PI3K/AKT signaling [19]. Collectively, we speculated that DAP12 may regulate TJ proteins through the PI3K/AKT pathway, thereby promoting the development of AKI.

In this study, we established AKI mouse models using cisplatin, and then assessed the expression levels of TJ proteins along with key markers of inflammation and oxidative stress. By establishing an AKI model in HK-2 cells with cisplatin, we determined the influence of DAP12 silencing on TJ proteins, inflammation, and oxidative stress. Accordingly, we identified a new mechanism through which the DAP12/PI3K/AKT pathway promoted the restoration of TJ protein expression levels, thereby reducing inflammation and oxidative stress in AKI. We anticipate that our findings will not only unveil novel therapeutic targets but also provide a fundamental theoretical framework for deepening our comprehension of AKI pathogenesis.

Materials and Methods

Mice

Thirty male C57BL/6 mice (Hua Fu Kang Co., China, 6 weeks old, 20–25 g) were housed in a specific pathogen-free facility under a 12-hour light/dark cycle, and received water and food *ad libitum*. All animal experiments conducted in this study were approved by the Ethics Committee for Experimental Animals Welfare in Zhejiang Center of Laboratory Animals (No. ZJCLA-IACUC-20030160).

Model of Cisplatin-Induced AKI

AKI was induced in mice by administration of cisplatin (purity >99.5%, Chengdu Herbpurify Co., Ltd., China) according to previous literature [20]. Mice were randomly distributed into a cisplatin-induced AKI model group (n = 6; intraperitoneal injection of cisplatin (20 mg/kg)) and a control group (n = 6; injection with an equal volume of saline). At 72 h after cisplatin injection, blood was collected from each mouse and centrifuged to obtain serum. Subsequently, all mice were anesthetized via an intraperitoneal injection of sodium pentobarbital (50 mg/kg) and euthanized by cervical dislocation. Kidney tissues were then immediately harvested and snap-frozen at –80 °C for subsequent analysis.

Histopathology Assessment

Kidney tissues were fixed in formalin, dehydrated in graded alcohol, embedded in paraffin, and sectioned at 4 µm. After deparaffinization using xylene, the sections were stained with hematoxylin (C0107, Beyotime, Shanghai, China) for 15 min and eosin (C0109, Beyotime, China) for 5 min, and mounted with neutral gum. The images were captured using a VECTRA 3 Quantitative Pathology Imaging System (PerkinElmer, Waltham, MA, USA) at $\times$100 magnification.

Biochemical Assay

The concentrations of blood urea nitrogen (BUN) and serum creatinine (SCr) that represent renal function were determined using the QuantiChrom Urea Assay Kit (DIUR-500, Bioassay Systems, Hayward, CA, USA) and Creatinine Assay Kit (DICT-500). Quantification of tumor necrosis factor-α (TNF-α) and interleukin-1β (IL-1β) inflammatory cytokines in cell culture supernatants and mouse serum was performed using the ELISA kit (ml077385, ml106733, mlbio, Shanghai, China; RK00027, RK00006, ABclonal, Wuhan, China). Additionally, mouse renal tubule tissues and HK-2 cells were dissolved in extraction buffer to detect malondialdehyde (MDA) level according to the manufacturer's instructions (A0003-1, Nanjing Jiancheng Bioengineering Institute, Nanjing, China).

Cell Culture and Transfection

HK-2 cells (AW-CELLS-H0142, Anweisci, Shanghai, China) were cultured in DMEM (Gibco, Grand Island, NY, USA) supplemented with 10% fetal bovine serum (12103C, Sigma-Aldrich, St. Louis, MO, USA), 1% penicillin-streptomycin (C0222, Beyotime, China), and 3 mM glutamine (37 °C, 5% CO_2). HK-2 cells were authenticated by short tandem repeat (STR) profiling and were tested negative for mycoplasma contamination. HK-2 cells were seeded into 24-well plates (2×10^4 cells/well) and randomly divided into the control (normally cultured cells), model (cisplatin-induced cell model), shNC, and

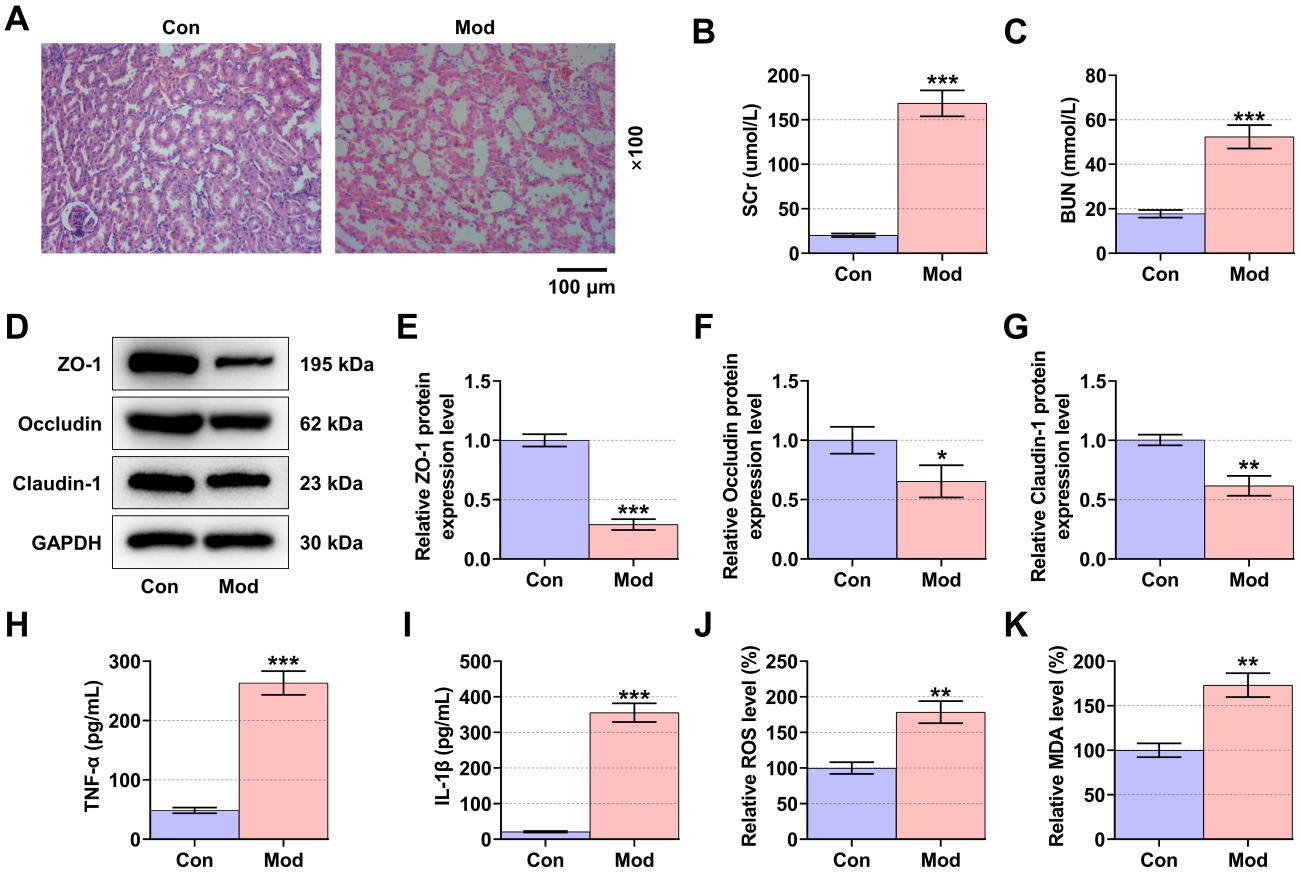

Fig. 1. Abnormalities of TJ proteins, inflammation, and oxidative stress in the AKI mouse model. (A) Representative micrographs showing the morphology of the kidneys from control and cisplatin-induced model groups (magnification, ×100). (B,C) Concentrations of serum creatinine and blood urea nitrogen. (D) Western blot results of ZO-1, Occludin, and Claudin-1 in the renal tubular tissue. (E–G) Quantitative analysis of ZO-1, Occludin, and Claudin-1 proteins. (H,I) Concentrations of TNF-α and IL-1β. (J,K) Relative levels of ROS and MDA. n = 6. TJ, tight junction; AKI, Acute kidney injury; MDA, Malondialdehyde; ROS, Reactive oxygen species; Con, Control; Mod, Model. A $p < 0.05$ was considered significant, *$p < 0.05$, **$p < 0.01$, ***$p < 0.001$ vs Con.

shDAP12 groups. The cells in the shDAP12 and shNC groups were transfected with short hairpin RNA targeting DAP12 (shDAP12) and corresponding controls shNC, respectively, utilizing Lipofectamine 2000 (11668500, Invitrogen, Camarillo, CA, USA). The shDAP12 sequence was 5′-TCAACACACAGAGGCCGTATT-3′, and the shNC sequence was 5′-TTCTCCGAACGTGTCACGT-3′. Control cells were exposed to an equivalent volume of phosphate buffer saline (PBS), and model cells were treated with 20 μM cisplatin for 18 h [20]. The cellular damage was observed under a light microscope. Later, cells were incubated with 3-(4,5-dimethyl-2-thiazolyl)-2,5-diphenyl-2-H-tetrazolium bromide (MTT, 5 mg/mL, C0009S, Beyotime, Shanghai, China) for an additional 4 h. Then, the supernatant was removed and formazan solution was added. The optical density was measured at 570 nm and cell viability was normalized as the percentage of control.

Reactive Oxygen Species (ROS) Measurement

HK-2 cells were incubated with 50 μM 2',7'-Dichlorodihydrofluorescein diacetate (DCFH-DA, D6883, Sigma-Aldrich, USA) (30 min) in the dark at 37 °C. Subsequently, the cells were washed twice with PBS to remove excess probe. The DCF fluorescence intensity was measured using a fluorescence microplate reader (Synergy H4 Hybrid, BioTek, Winooski, VT, USA) with an excitation wavelength of 504 nm and an emission wavelength of 529 nm. Relative ROS levels were derived from the fluorescence intensity data, expressed by normalizing the mean fluorescence intensity of each treatment group to that of the control group.

Western Blotting

Total protein was isolated from mouse renal tubule tissues or cells using RIPA buffer containing a phosphatase inhibitor, protease inhibitor, and phenylmethylsulfonyl fluoride (PMSF). The bicinchoninic acid (BCA) Protein Assay kit was utilized to quantify the protein

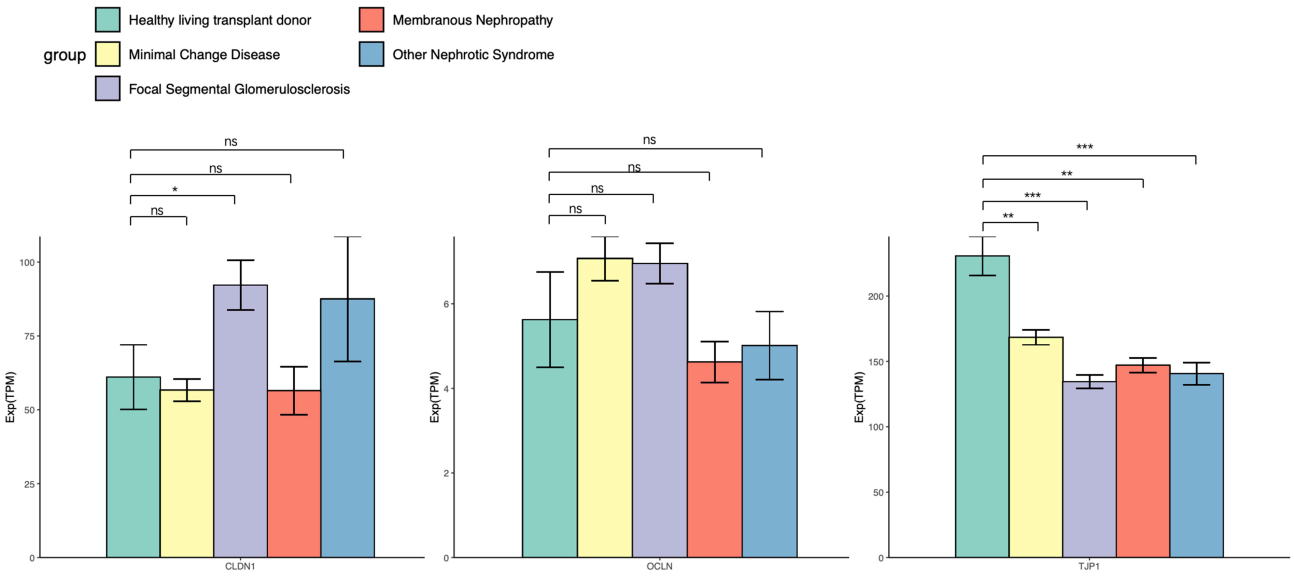

Fig. 2. Expression of three TJ proteins in kidney injury-related diseases. TJP1, tight junction protein 1; CLDN1, Claudin-1; OCLN, Occludin. ns, not significant. *$p < 0.05$, **$p < 0.01$, ***$p < 0.001$ vs Healthy living transplant donor.

concentrations. Next, the proteins were separated using 12% SDS-PAGE (P0012A, Beyotime, China) and transferred onto a polyvinylidene difluoride membrane (FFP19, Beyotime, China). The membrane was incubated with primary antibodies at 4 °C overnight, incorporating glyceraldehyde-3-phosphate dehydrogenase (GAPDH, 1:5000; ab9485, Abcam, Cambridge, UK), ZO1 (1:1000, ab276131, Abcam), Occludin (1:1000; ab216327; Abcam), Claudin 1 (1:1000; ab307692; Abcam), DAP12 (1:1000; ab280568; Abcam), PI3 Kinase p85 alpha (phospho Y467) + PI3 Kinase p55 (phospho Y199) (0.5 μg/mL; ab278545; Abcam), PI3 Kinase catalytic subunit gamma/PI3K-gamma (1:1000, ab302958, Abcam), AKT (phospho T308) (1:1000, ab38449, Abcam), and pan-AKT (1:1000, ab8805, Abcam). Then the membrane was incubated with secondary antibodies (1:5000, ab205718, Abcam) at room temperature for 1 h, followed by treatment with SuperSignal ECL (ThermoFisher Scientific, Waltham, MA, USA) and visualization using a UVP imaging system (Upland, CA, USA). The images obtained were analyzed utilizing ImageJ software (version 1.52p, NIH, Bethesda, MD, USA), and the gray densities of protein bands were normalized employing GAPDH density as the internal control.

Bioinformatics Analysis

Using the Gene Expression Omnibus database GSE254957 [21], which includes RNA sequencing data from 282 glomerulus samples derived from healthy living transplant donors, focal segmental glomerulosclerosis, membranous nephropathy, disease with minimal changes, other nephrotic syndromes, and other phenotypes, the expression levels of three TJ proteins (ZO-1, Occludin, Claudin-1) were assessed in kidney injury-related diseases. Gene sets positively and negatively correlated with TJP1 were determined using WGCNA, followed by Gene Ontology (GO) and Kyoto Encyclopedia of Genes and Genomes (KEGG) enrichment analyses, as well as PPI analysis, to identify genes and signaling pathways closely related to TJ protein expression. WGCNA was performed to construct a scale-free network with an optimal soft-threshold power of 7. In the gene significance (GS)-gene significance (MM) analysis, core genes were selected using thresholds of GS >0.8 and MM >0.2. GO and KEGG enrichment analyses were performed using the clusterProfiler package [22]. The PPI network of MitoDEGs was retrieved from the String database [23] and analyzed using Cytoscape [24]. Core genes were screened based on degree values and the maximal clique centrality (MCC) method implemented in the cytoHubba plugin.

Statistical Analysis

Statistical analysis was performed using GraphPad Prism software version 8.0 (GraphPad Software Inc., San Diego, CA, USA). Data are expressed as mean $\pm$ standard deviation. Independent samples *t*-test was employed for two-group comparison, while one-way ANOVA with Tukey's test was applied for multi-group comparison. A $p < 0.05$ was considered statistically significant. * or ^ indicated $p < 0.05$, ** or ^^ indicated $p < 0.01$, and *** or ^^^ indicated $p < 0.001$.

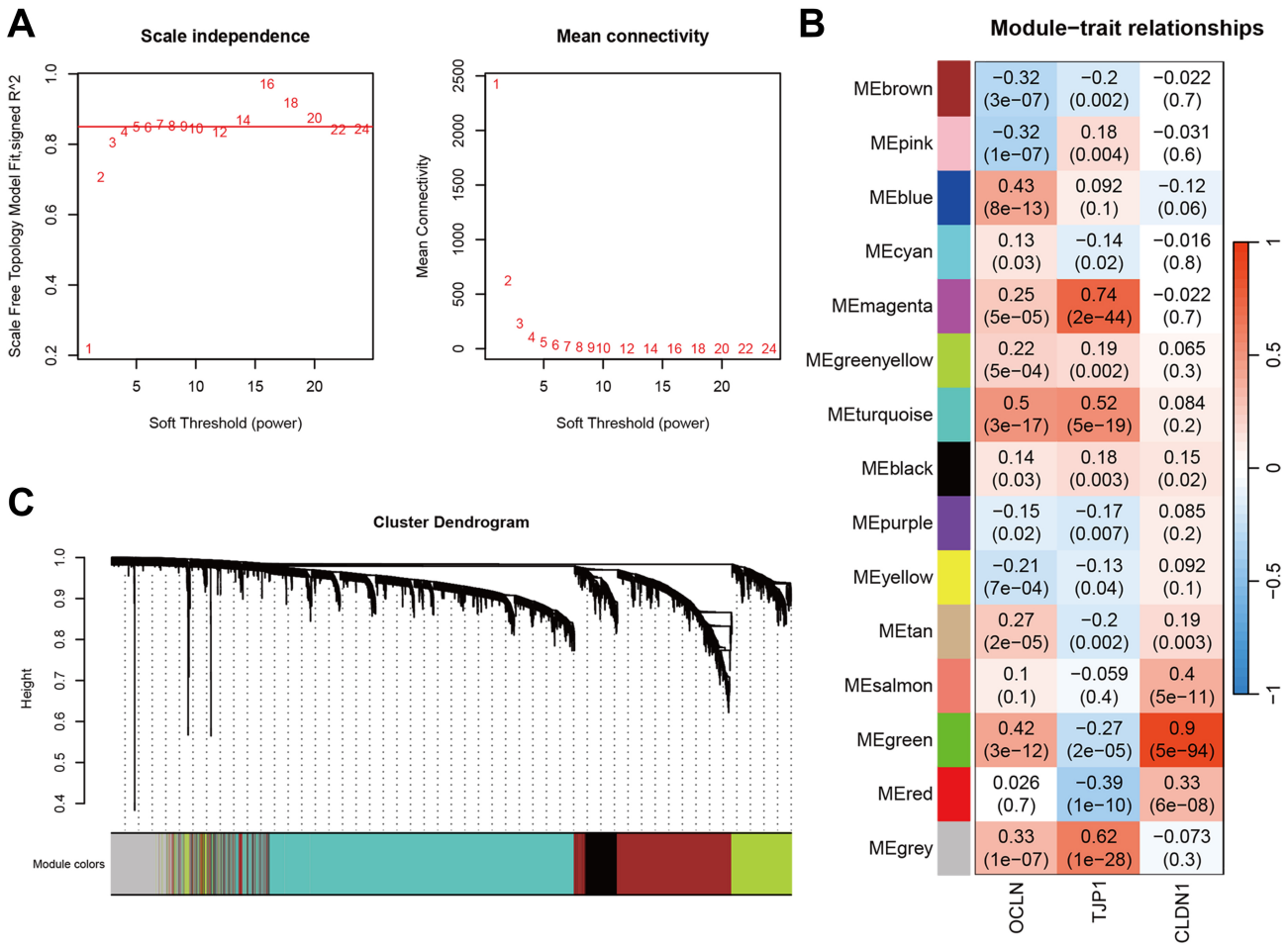

Fig. 3. Identification of targets associated with TJ protein downregulation using WGCNA. (A) The best soft-threshold power. (B) Module-TJs correlative analysis. Each row and column corresponds to a module eigengene and different TJs, respectively. Heatmap block with correlation coefficients and *p*-values. (C) Clustering dendrogram of genes, with dissimilarity based on topological overlap. TJs, tight junctions; WGCNA, Weighted Gene Co-Expression Network Analysis.

Results

Abnormalities of TJ Proteins, Inflammation, and Oxidative Stress in a Cisplatin-Induced AKI Model

To explore whether inflammation and oxidative stress were associated with TJ proteins in AKI, we first established a mouse model of AKI by administration of cisplatin. H&E staining results revealed significant pathological changes in the kidney tissue of cisplatin-treated mice, manifested by irregular cell structure, necrosis, and the shedding of renal tubular epithelial cells (Fig. 1A). Additionally, BUN and SCr levels were significantly elevated in AKI model mice ($p < 0.001$, Fig. 1B,C), while levels of TJ proteins (Claudin-1, ZO-1, and Occludin) were markedly downregulated in the renal tubular tissue (Fig. 1D,E, $p < 0.001$; Fig. 1F, $p < 0.05$; Fig. 1G, $p < 0.01$). ELISA data showed remarkable upregulation of inflammatory cytokines IL-1β and TNF-α in the serum from AKI model mice ($p < 0.001$, Fig. 1H,I). Oxidative stress markers, including ROS and MDA, were quantified in the renal tubular tissue, and their levels were significantly upregulated in AKI model mice ($p < 0.01$, Fig. 1J,K). These results suggest abnormal levels of inflammation, oxidative stress, and TJ proteins in AKI model mice.

Identification of Targets Associated With TJ Protein Downregulation Using WGCNA

We performed a WGCNA to identify key candidate genes associated with the downregulation of TJ proteins for further investigation. Bioinformatics screening revealed that among the three TJ proteins (ZO-1, Occludin, Claudin-1), only TJP1 (also known as ZO-1) level decreased in kidney injury-related diseases, while the other two showed no significant changes ($p < 0.01$, Fig. 2). The soft-threshold power was calibrated to 7 (scale-free $R^2 = 0.85$) through WGCNA (Fig. 3A). The results showed that genes in the Magenta, Turquoise, and grey modules were strongly positively correlated with OCLN expression (Fig. 3B). In addition, gene sets showed a strong positive correlation with TJP1 expression, including genes in

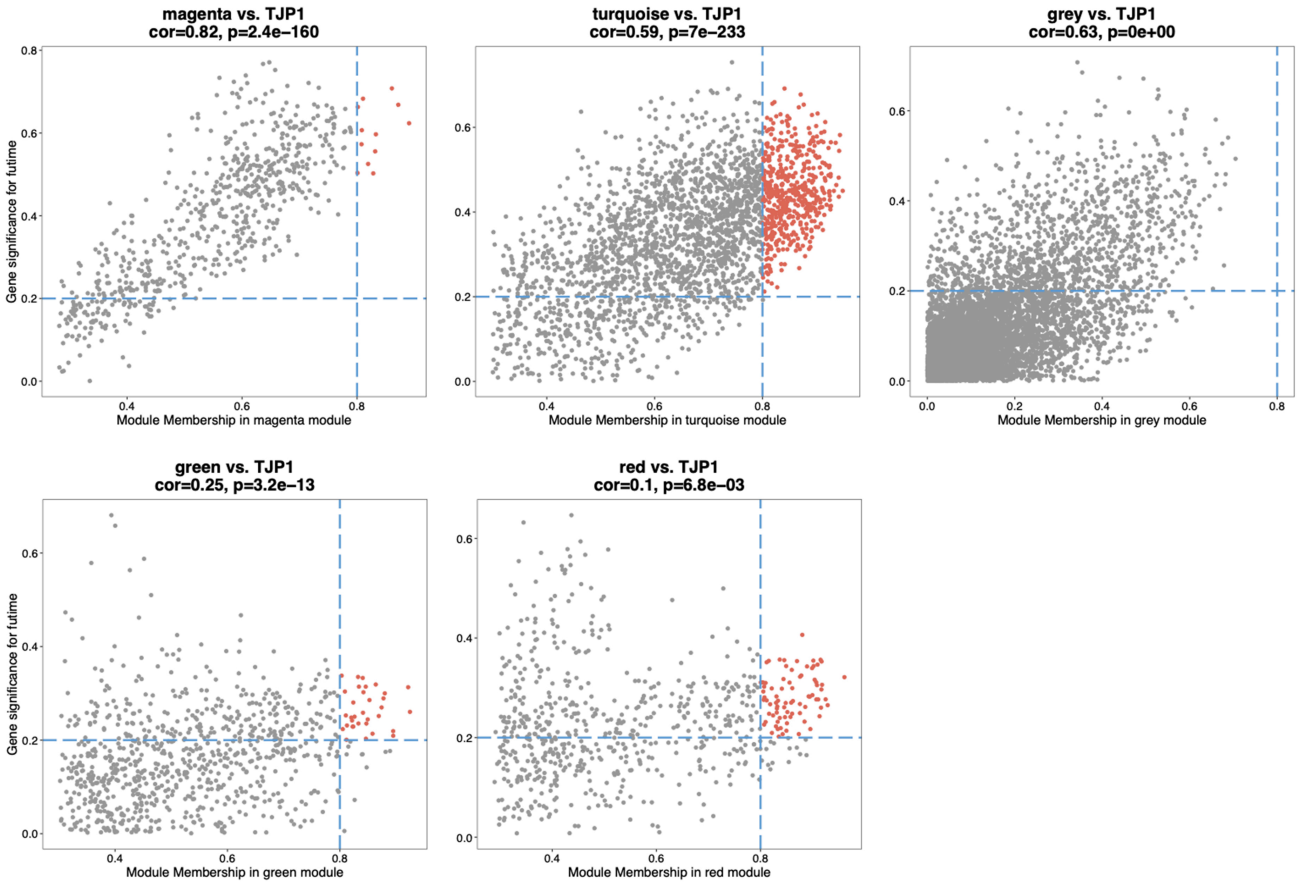

Fig. 4. Correlation analysis of the Magenta, Turquoise, Grey, Red and Green modules with the TJP1 expression. TJP1, tight junction protein 1.

the Magenta, Turquoise, and grey modules. Conversely, genes in the green and red modules were negatively correlated with TJP1 expression (Fig. 3B). Fig. 3C shows the clustering dendrogram of genes based on topological overlap, along with assigned merged module colors and original module colors. These TJP1-correlated modules were subsequently subjected to downstream functional analysis and central regulator screening. To further explore genes highly correlated with TJP1 expression in these modules, we performed a correlation analysis between module membership (MM) and gene significance (GS) (Fig. 4).

GO and KEGG Enrichment Analyses on Differentially Expressed Genes (DEGs)

To elucidate the biological functions of the genes, particularly those negatively correlated with TJP1, we performed GO and KEGG enrichment analyses on the DEGs derived from the relevant modules. GO enrichment analysis results revealed that the negatively correlated DEGs were prominently enriched in immunity-related categories, such as the immune response-regulating signaling pathway, positive regulation of immune effector process, and signaling pathway regulation of immune effector process (Fig. 5A,B). KEGG enrichment analysis data unraveled that negatively correlated DEGs were markedly enriched in the B cell receptor signaling pathway, Natural killer cell-mediated cytotoxicity, and Neutrophil extracellular trap formation (Fig. 6A,B).

Identification of the TYROBP/DAP12-PI3K-AKT Pathway as a Core Module

We constructed a PPI network to pinpoint a central regulator from this enriched gene set. Then, TYROBP, also known as DAP12, was identified as a core gene among the negatively correlated genes (Figs. 7,8); hence, it was established as a key candidate for subsequent experimental validation. To validate the activity of this identified pathway in our experimental model, we assessed its expression levels. Western blot analysis results demonstrated a notable upregulation of DAP12, and elevated ratios of p-PI3K/PI3K and p-AKT/AKT in the renal tubular tissue of AKI model mice ($p < 0.001$, Fig. 9A–D), denoting an evident activation of the TYROBP/PI3K/AKT pathway in the kidney injury model.

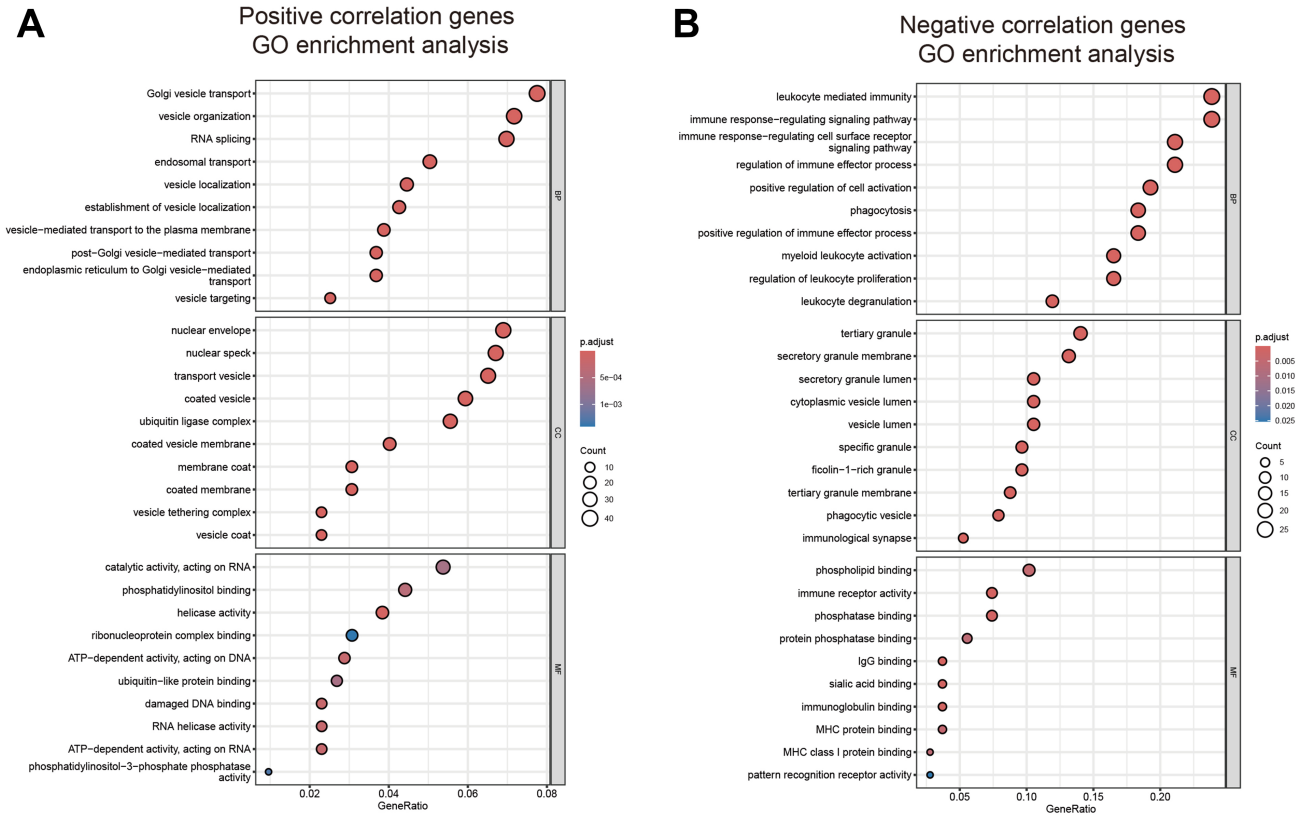

Fig. 5. GO enrichment analyses of DEGs. (A,B) A bubble plot depicting GO enrichment analyses results. GO, Gene Ontology; DEGs, differentially expressed genes.

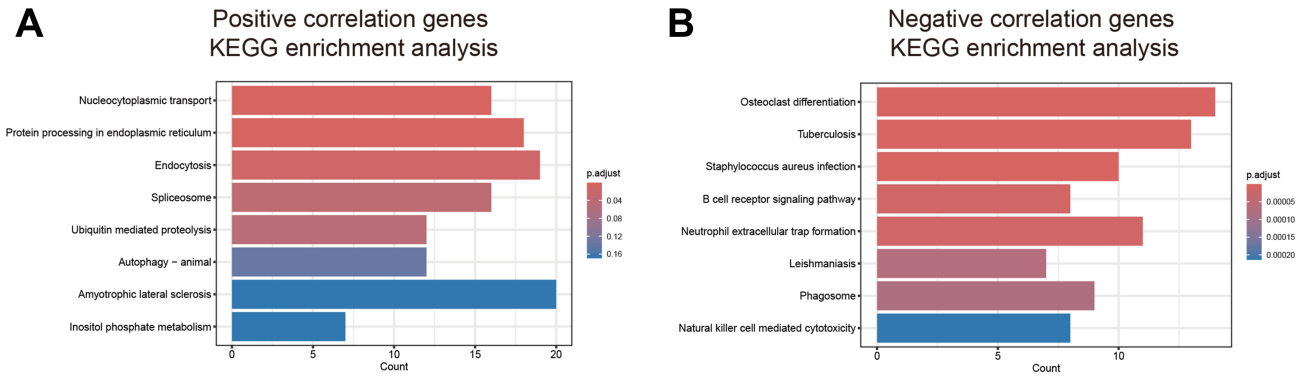

Fig. 6. KEGG enrichment analyses of DEGs. (A,B) A bar chart presenting KEGG enrichment analyses results. KEGG, Kyoto Encyclopedia of Genes and Genomes; DEGs, differentially expressed genes.

The Mitigating Effect of DAP12 Silencing on Renal Tubular Epithelial Cell Injury

We established a cisplatin-induced cell injury model using renal tubular epithelial cells, HK-2. Based on bioinformatics analysis data, shDAP12 was constructed and demonstrated by Western blotting to cause the loss of DAP12 in model cells ($p < 0.001$, Fig. 10A,B). After silencing of DAP12 in HK-2 cells, cellular damage was observed under a light microscope, revealing significantly mitigated cell injury ($p < 0.01$, Fig. 10C,D). Furthermore, in the HK-2 cell model, there was remarkable downregulation of TJ proteins ZO-1, Claudin-1, and Occludin (Fig. 10E,F, $p < 0.001$; Fig. 10G, $p < 0.01$; Fig. 10H, $p < 0.001$), yet DAP12 silencing markedly reversed the downregulation of Claudin-1 and ZO-1 ($p < 0.001$, Fig. 10E,F,H). Occludin expression was increased after DAP12 silencing, but without a statistically significant difference (Fig. 10G). Meanwhile, ELISA results revealed the upregulation of inflammatory cytokines IL-1β and TNF-α in the cell injury model, and this upregulation was suppressed by DAP12 silencing ($p < 0.001$, Fig. 10I,J). DAP12 silencing also decreased levels of two oxidative stress indicators, MDA and ROS ($p <$

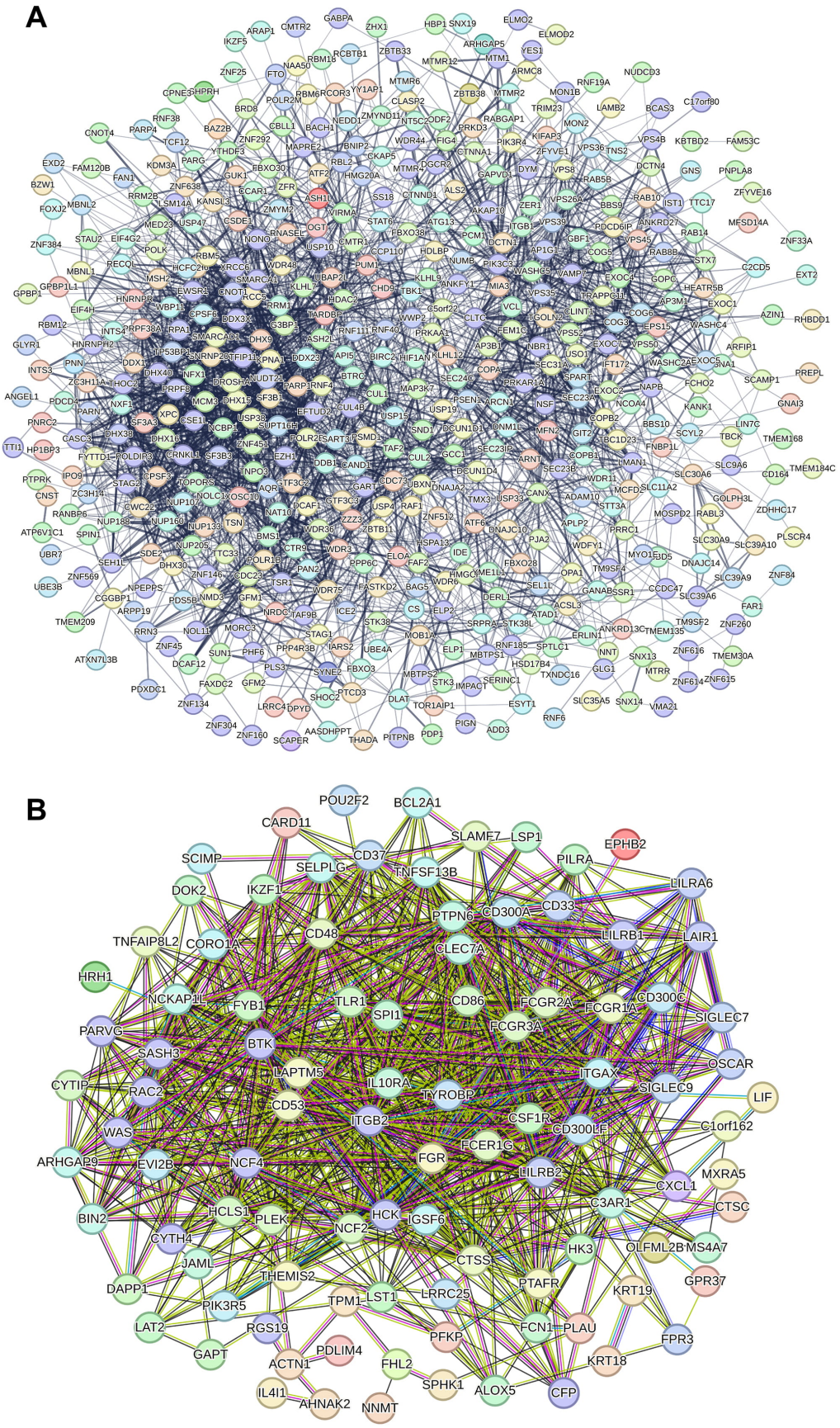

Fig. 7. Screening hub genes by PPI network analysis. (A) PPI network analysis of positively correlated genes. (B) PPI network analysis of negatively correlated genes. PPI, Protein-Protein Interaction.

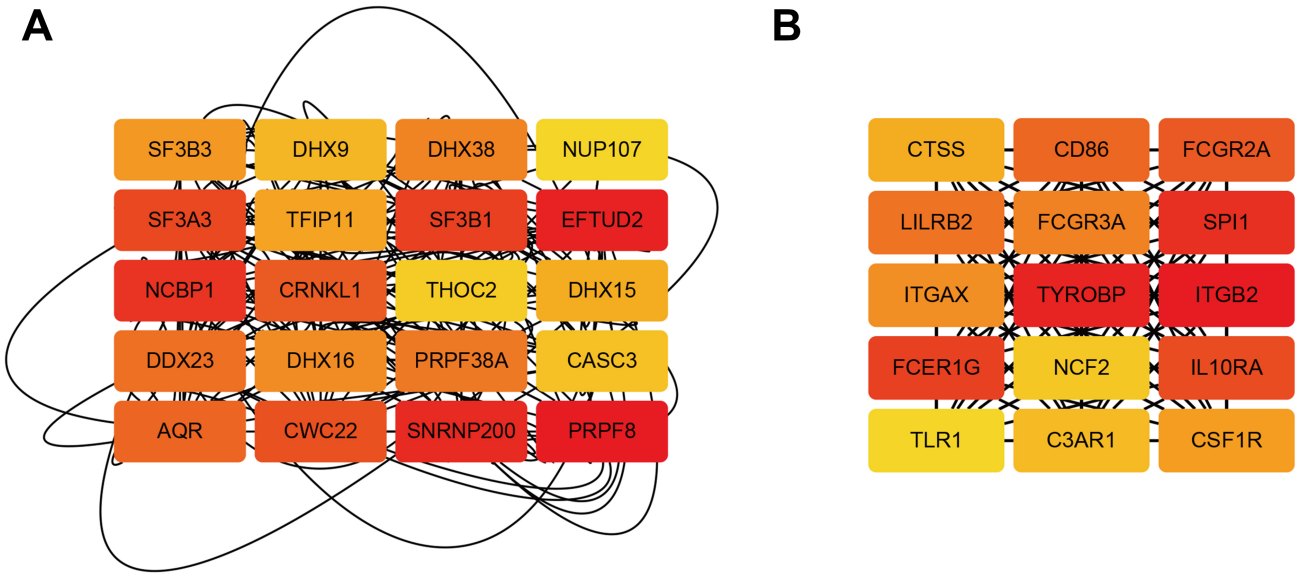

Fig. 8. Screening hub genes by PPI network analysis. (A) PPI network analysis of the positively correlated core gene. (B) PPI network analysis of the negatively correlated core gene. PPI, Protein-Protein Interaction.

0.01, Fig. 11A,B). Subsequently, we observed a significant inhibition of p-PI3K and p-AKT activation upon DAP12 silencing ($p < 0.001$, Fig. 11C–E), indicating that DAP12 may affect the pathogenesis of AKI by upregulating the PI3K/AKT pathway.

Discussion

This study delved into the associations between inflammation, oxidative stress, and TJ proteins in AKI using a cisplatin-induced AKI mouse model and an HK-2 cell injury model. Our results indicated that in the AKI mouse model, kidney tissues, particularly the renal tubules, exhibited evident pathological changes accompanied by significant renal dysfunction. Levels of TJ proteins (ZO-1, Claudin-1 and Occludin) were downregulated, together with markedly upregulated inflammatory cytokines (IL-1β and TNF-α) and oxidative stress markers (MDA and ROS), analogous to previous findings [25,26]. Furthermore, the concurrent abnormalities in TJ protein expression, inflammation and oxidative stress in AKI suggested a potential close association among these factors.

A previous study has reported that kidney damage leads to a decrease in the expression level of ZO-1 [27]. Through bioinformatics analysis, we discovered that among the three TJ proteins, only the TJP1 (ZO-1) level was downregulated in kidney injury-related diseases. Consequently, we further explored genes highly correlated with TJP1 expression. GO/KEGG enrichment analyses of these DEGs revealed that negatively correlated genes were primarily enriched in immunity-related categories, among which TYROBP (DAP12) was identified as the core gene using PPI network analysis. As reported, DAP12 plays a crucial role in immune responses and is associated with multiple signaling pathways [28,29]. Based on transcriptomics technology, TYROBP has been identified as a new macrophage-related biomarker for the diagnosis of AR after kidney transplantation [30]. DAP12 also participates in renal inflammation during unilateral ureter obstruction progression through activating a receptor, triggering receptor expressed on myeloid cell (TREM) [31]. Deletion of DAP12-coupled receptor LMIR5 improves acute tubular necrosis and cast formation, and inhibits neutrophil recruitment [32]. In rheumatoid arthritis, tyrosine in the ITAM motif of DAP12 is phosphorylated, inducing recruitment of Syk tyrosine kinase and ultimately activating PI3 kinase and ERK signaling pathways, and inhibition of DAP12 signaling pathway can deactivate important inflammatory cells [18]. Moreover, DAP12 expression is upregulated in renal ischemia-reperfusion injury and in hypoxia-treated HK-2 cells, positioning it as a prominent candidate gene related to the "acute renal failure" pathway [15]. Herein, we confirmed apparent upregulation of DAP12 in the AKI mouse model, which was closely pertinent to activated PI3K/AKT signaling pathway. This implied that DAP12 may affect the expression and function of TJP1 by regulating the PI3K/AKT signaling pathway, thus participating in the pathogenesis of AKI.

To further validate this hypothesis, DAP12 was silenced in a cisplatin-induced HK-2 cell injury model. DAP12 silencing mitigated cell injury, upregulated Claudin-1 and ZO-1 levels, and significantly downregulated levels of inflammatory cytokines (IL-1β and TNF-α) and oxidative stress markers (MDA and ROS), whereas the level of Occludin was not statistically significant. Notably, silencing of DAP12 also inactivated PI3K/AKT signaling pathway that is instrumental in cell proliferation, apoptosis,

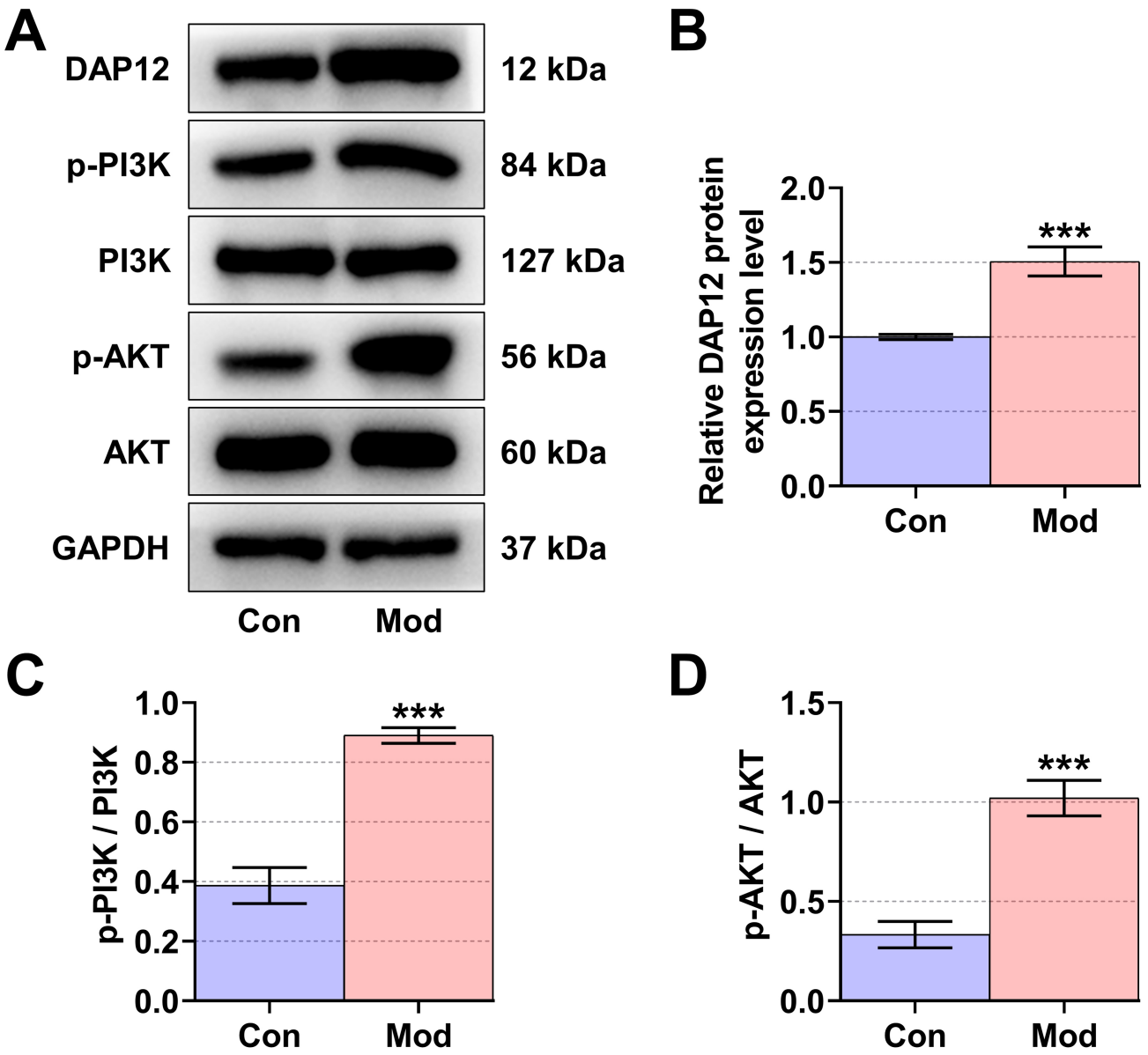

Fig. 9. The activation of the DAP12/PI3K/AKT signaling pathway in cisplatin-induced model mice. (A) Western blot results of DAP12, p-PI3K, P13K, p-AKT, and AKT in the renal tubular tissue. (B–D) Quantitative analysis of protein levels of DAP12, p-PI3K/P13K, and p-AKT/AKT. n = 6. Con, Control; Mod, Model. A $p < 0.05$ was considered significant, ***$p < 0.001$ vs Con.

and metabolism [33,34]. The deficiency of p-PI3K and p-Akt can promote the expression of ZO-1 and Claudin-5, thereby mitigating blood-brain barrier disruption [15]. Moreover, Butyrate enhances the expression levels of ZO-1, Cadherin-1, and Occludin in HK-2 cells via inactivation of PI3K/Akt pathway, thus maintaining the TJ structure of renal tubular epithelial cells, and attenuating renal tissue fibrosis [19]. Arbutin improves renal function, reduces inflammation and apoptosis, and alleviates LPS-induced AKI through modulating the PI3K/Akt/Nrf2 pathway *in vivo* [35]. Therefore, silencing DAP12 to blunt PI3K/AKT activation, upregulate TJP1, and ameliorate inflammation and oxidative stress, may represent a promising therapeutic strategy for AKI.

While these findings highlight the potential therapeutic value of targeting the DAP12/PI3K/AKT axis in AKI, there are limitations that must be considered. Firstly, this study mainly focused on gene and protein levels, lacking multidimensional data for a comprehensive pathophysiological insight into AKI. Secondly, whether DAP12 directly binds to the TJ protein or regulates its transcription still requires further validation. Thirdly, the reliance on animal and cell models necessitates caution when extrapolating these results to human AKI, due to interspecies differences in immune responses, renal regenerative capacity, and the specific modeled etiology (cisplatin) compared with the diverse clinical causes (e.g., sepsis, ischemia-reperfusion). Fourthly, the initial bioinformatic identification of DAP12

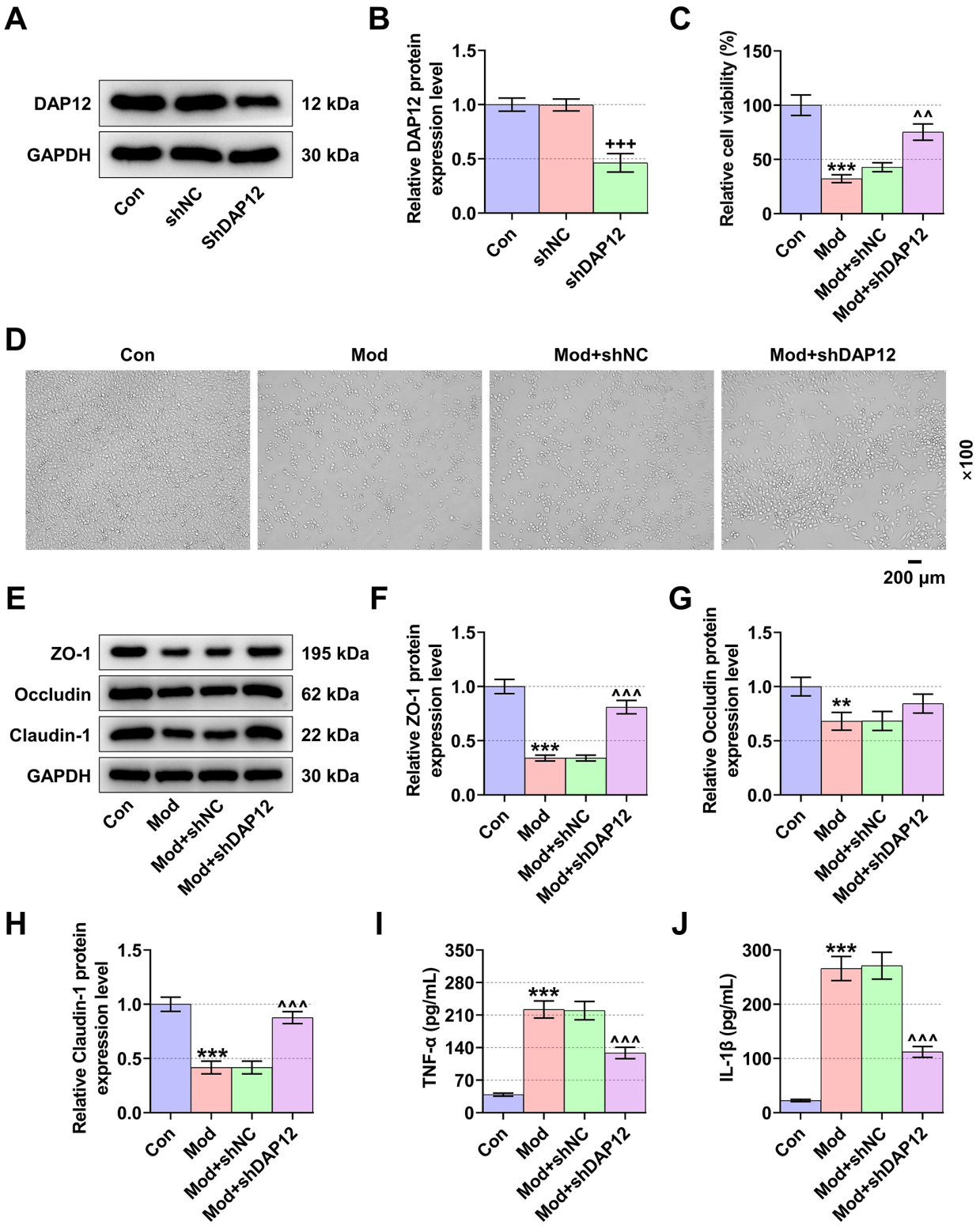

Fig. 10. The mitigating effect of DAP12 silencing on cisplatin-induced HK-2 cell injury. (A) Western blot results of DAP12. (B) Quantitative analysis of DAP12 protein level. (C) MTT assay results of HK-2 cell viability in each group. (D) Morphology and cellular damage of HK-2 cells across treatment groups under light microscopy. (E) Western blot results of ZO-1, Occludin, and Claudin-1. (F–H) Quantitative analysis of protein levels of ZO-1, Occludin, and Claudin-1. (I,J) Concentrations of TNF-α and IL-1β. Data are expressed as mean ± SD from three independent biological replicates (n = 3). MTT, 3-(4,5-dimethyl-2-thiazolyl)-2,5-diphenyl-2-H-tetrazolium bromide; Con, Control; Mod, Model. A $p < 0.05$ was considered significant, $^{+++}p < 0.001$ vs shNC; $^{**}p < 0.01$, $^{***}p < 0.001$ vs Con; $^{\wedge\wedge}p < 0.01$, $^{\wedge\wedge\wedge}p < 0.001$ vs Mod+shNC.

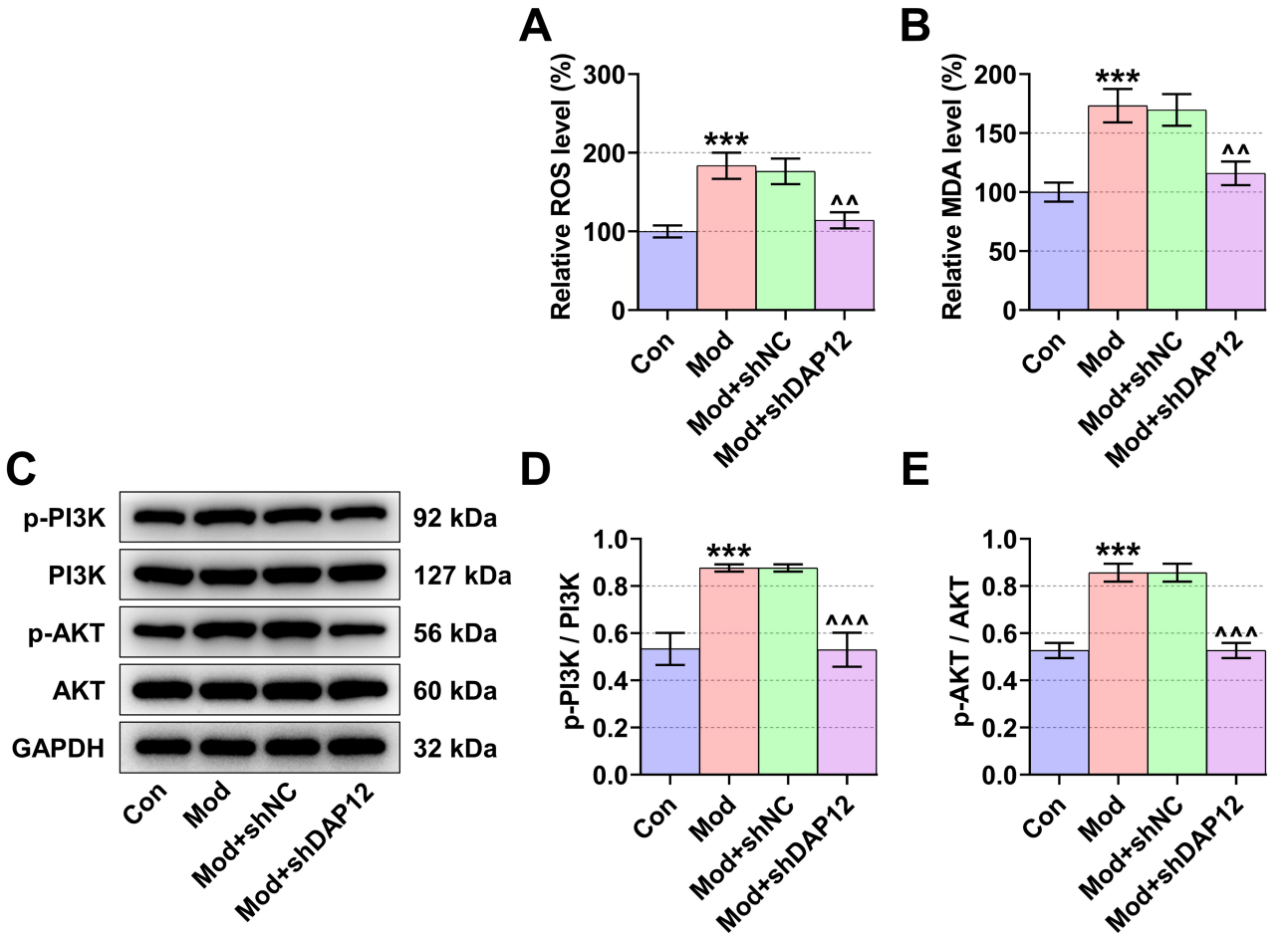

Fig. 11. Inhibiting effects of DAP12 silencing on inflammation, oxidative stress, and the activation of PI3K/AKT signaling pathway. (A,B) Relative levels of ROS and MDA. (C) Western blot results of p-PI3K, P13K, p-AKT and AKT. (D,E) Quantitative analysis of protein levels of p-PI3K/P13K and p-AKT/AKT. Data are expressed as mean ± SD from three independent biological replicates (n = 3). A $p < 0.05$ was considered significant, ***$p < 0.001$ vs Con; $^{\wedge\wedge}p < 0.01$, $^{\wedge\wedge\wedge}p < 0.001$ vs Mod+shNC.

was based on a glomerular dataset (GSE254957), whereas this study focuses on tubular injury. Although subsequent validation confirmed its role in tubular models, the cross-compartmental origin of this candidate gene should be acknowledged. Therefore, the role of the DAP12/PI3K/AKT pathway in AKI discovered in this study and its potential as a therapeutic target warrant further verification in human samples and more clinical models. To bridge the gap between our fundamental findings and their potential clinical utility, future research can focus on several translational directions, such as verifying the role of DAP12 in human AKI samples, conducting mechanism and therapeutic research using human organoids or humanized models, deeply analyzing the upstream and downstream regulatory mechanisms of DAP12 in human kidney cells, developing and optimizing safe and efficient targeting strategies, and exploring the potential of DAP12 as a biomarker for AKI.

Conclusion

In summary, our study demonstrates that DAP12 plays a critical role in AKI pathogenesis. DAP12 silencing effectively suppresses the activation of the PI3K/AKT pathway, upregulates TJP1 expression, and subsequently ameliorates inflammation and oxidative stress, thereby preserving renal barrier function. These findings not only identify DAP12 as a key gene negatively correlated with TJ1 but also highlight the therapeutic potential of targeting the DAP12/PI3K/AKT axis. Future studies on the upstream regulators and downstream effectors of DAP12 will be essential, as a deeper mechanistic understanding is expected to pave the way for developing more precise and effective strategies for the clinical prevention and treatment of AKI.

Availability of Data and Materials

The datasets used or analyzed during the current study are available from the corresponding author upon reasonable request.

Author Contributions

YZ: Conceptualization, Validation, Writing - original draft, Writing - review & editing. HS: Data curation, Formal analysis, Writing - original draft, Writing - review & editing. JW: Investigation, Visualization, Writing - original draft, Writing - review & editing. TL: Formal analysis, Methodology, Software, Writing - original draft, Writing - review & editing. PQ: Formal analysis, Validation, Writing - original draft, Writing - review & editing. WZ: Data curation, Project administration, Supervision, Writing - original draft, Writing - review & editing. All authors gave final approval of the version to be published. All authors have participated sufficiently in the work to take public responsibility for appropriate portions of the content and agreed to be accountable for all aspects of the work in ensuring that questions related to its accuracy or integrity.

Ethics Approval and Consent to Participate

All animal experiments conducted in this study were approved by the Ethics Committee for Experimental Animals Welfare in Zhejiang Center of Laboratory Animals (No. ZJCLA-IACUC-20030160).

Acknowledgment

Not applicable.

Funding

This research received no external funding.

Conflict of Interest

The authors declare no conflict of interest.

References

[1] Turgut F, Awad AS, Abdel-Rahman EM. Acute Kidney Injury: Medical Causes and Pathogenesis. Journal of Clinical Medicine. 2023; 12: 375. https://doi.org/10.3390/jcm12010375.

[2] Guo C, Dong G, Liang X, Dong Z. Epigenetic regulation in AKI and kidney repair: mechanisms and therapeutic implications. Nature Reviews. Nephrology. 2019; 15: 220–239. https://doi.org/10.1038/s41581-018-0103-6.

[3] Singbartl K, Kellum JA. AKI in the ICU: definition, epidemiology, risk stratification, and outcomes. Kidney International. 2012; 81: 819–825. https://doi.org/10.1038/ki.2011.339.

[4] Sato Y, Yanagita M. Immune cells and inflammation in AKI to CKD progression. American Journal of Physiology. Renal Physiology. 2018; 315: F1501–F1512. https://doi.org/10.1152/ajprenal.00195.2018.

[5] Pais T, Jorge S, Lopes JA. Acute Kidney Injury in Sepsis. International Journal of Molecular Sciences. 2024; 25: 5924. https://doi.org/10.3390/ijms25115924.

[6] Andrianova NV, Zorov DB, Plotnikov EY. Targeting Inflammation and Oxidative Stress as a Therapy for Ischemic Kidney Injury. Biochemistry. Biokhimiia. 2020; 85: 1591–1602. https://doi.org/10.1134/S0006297920120111.

[7] Oliveira BM, de Almeida LF, Deluque AL, Souza CS, Maciel ALD, Francescato HDC, *et al*. Calcitriol Reduces the Inflammation, Endothelial Damage and Oxidative Stress in AKI Caused by Cisplatin. International Journal of Molecular Sciences. 2022; 23: 15877. https://doi.org/10.3390/ijms232415877.

[8] Ow CPC, Trask-Marino A, Betrie AH, Evans RG, May CN, Lankadeva YR. Targeting Oxidative Stress in Septic Acute Kidney Injury: From Theory to Practice. Journal of Clinical Medicine. 2021; 10: 3798. https://doi.org/10.3390/jcm10173798.

[9] Kuo WT, Odenwald MA, Turner JR, Zuo L. Tight junction proteins occludin and ZO-1 as regulators of epithelial proliferation and survival. Annals of the New York Academy of Sciences. 2022; 1514: 21–33. https://doi.org/10.1111/nyas.14798.

[10] Szaszi K, Amoozadeh Y. New insights into functions, regulation, and pathological roles of tight junctions in kidney tubular epithelium. International Review of Cell and Molecular Biology. 2014; 308: 205–271. https://doi.org/10.1016/B978-0-12-800097-7.00006-3.

[11] Lee DBN, Huang E, Ward HJ. Tight junction biology and kidney dysfunction. American Journal of Physiology. Renal Physiology. 2006; 290: F20–F34. https://doi.org/10.1152/ajprenal.00052.2005.

[12] Eadon MT, Hack BK, Xu C, Ko B, Toback FG, Cunningham PN. Endotoxemia alters tight junction gene and protein expression in the kidney. American Journal of Physiology. Renal Physiology. 2012; 303: F821–F830. https://doi.org/10.1152/ajprenal.00023.2012.

[13] Wei W, Li W, Yang L, Weeramantry S, Ma L, Fu P, *et al*. Tight junctions and acute kidney injury. Journal of Cellular Physiology. 2023; 238: 727–741. https://doi.org/10.1002/jcp.30976.

[14] Trujillo J, Molina-Jijón E, Medina-Campos ON, Rodríguez-Muñoz R, Reyes JL, Loredo ML, *et al*. Renal tight junction proteins are decreased in cisplatin-induced nephrotoxicity in rats. Toxicology Mechanisms and Methods. 2014; 24: 520–528. https://doi.org/10.3109/15376516.2014.948248.

[15] Grigoryev DN, Cheranova DI, Heruth DP, Huang P, Zhang LQ, Rabb H, *et al*. Meta-analysis of molecular response of kidney to ischemia reperfusion injury for the identification of new candidate genes. BMC Nephrology. 2013; 14: 231. https://doi.org/10.1186/1471-2369-14-231.

[16] Pei J, Zhang J, Yu C, Luo J, Wen S, Hua Y, *et al*. Transcriptomics-based exploration of shared M1-type macrophage-related biomarker in acute kidney injury after kidney transplantation and acute rejection after kidney transplantation. Transplant Immunology. 2024; 85: 102066. https://doi.org/10.1016/j.trim.2024.102066.

[17] Han Y, Wang L, Ye X, Gong X, Shao X. FcγRIIb Exacerbates LPS-Induced Neuroinflammation by Binding with the Bridging Protein DAP12 and Promoting the Activation of PI3K/AKT Signaling Pathway in Microglia. Journal of Inflammation Research. 2024; 17: 41–57. https://doi.org/10.2147/JIR.S428093.

[18] Chen X, Eksioglu EA, Carter JD, Fortenbery N, Donatelli SS, Zhou J, *et al*. Inactivation of DAP12 in PMN inhibits TREM1-mediated activation in rheumatoid arthritis. PloS One. 2015; 10: e0115116. https://doi.org/10.1371/journal.pone.0115116.

[19] Sun X, Xi Y, Yan M, Sun C, Tang J, Dong X, *et al*. *Lactiplantibacillus* plantarum NKK20 Increases Intestinal Butyrate Production and Inhibits Type 2 Diabetic Kidney Injury through PI3K/Akt Pathway. Journal of Diabetes Research. 2023; 2023: 8810106. https://doi.org/10.1155/2023/8810106.

[20] Chen X, Wei W, Li Y, Huang J, Ci X. Hesperetin relieves cisplatin-induced acute kidney injury by mitigating oxidative stress, inflammation and apoptosis. Chemico-biological Interactions. 2019; 308: 269–278. https://doi.org/10.1016/j.cbi.2019.05.040.

[21] Sealfon R, Mariani L, Avila-Casado C, Nair V, Menon R, Funk J, *et al*. Molecular Characterization of Membranous Nephropathy. Journal of the American Society of Nephrology: JASN. 2022; 33: 1208–1221. https://doi.org/10.1681/ASN.2021060784.

[22] Yu G, Wang LG, Han Y, He QY. clusterProfiler: an R package for comparing biological themes among gene clusters. Omics: a Journal of Integrative Biology. 2012; 16: 284–287. https://doi.org/10.1089/omi.2011.0118.

[23] Snel B, Lehmann G, Bork P, Huynen MA. STRING: a web-server to retrieve and display the repeatedly occurring neighbourhood of a gene. Nucleic Acids Research. 2000; 28: 3442–3444. https://doi.org/10.1093/nar/28.18.3442.

[24] Shannon P, Markiel A, Ozier O, Baliga NS, Wang JT, Ramage D, *et al*. Cytoscape: a software environment for integrated models of biomolecular interaction networks. Genome Research. 2003; 13: 2498–2504. https://doi.org/10.1101/gr.1239303.

[25] Ji Y, Xiao Y, Li S, Fan Y, Cai Y, Yang B, *et al*. Protective effect and mechanism of Xiaoyu Xiezhuo decoction on ischemia-reperfusion induced acute kidney injury based on gut-kidney crosstalk. Renal Failure. 2024; 46: 2365982. https://doi.org/10.1080/0886022X.2024.2365982.

[26] Lou Y, Shi H, Sha N, Li F, Gu X, Lin H. Ursodeoxycholic acid protects against sepsis-induced acute kidney injury by activating Nrf2/HO-1 and inhibiting NF-κB pathway. BMC Nephrology. 2025; 26: 45. https://doi.org/10.1186/s12882-025-03977-9.

[27] Zhou X, Zang X, Guan Y, Tolbert T, Zhao TC, Bayliss G, *et al*. Targeting enhancer of zeste homolog 2 protects against acute kidney injury. Cell Death & Disease. 2018; 9: 1067. https://doi.org/10.1038/s41419-018-1012-0.

[28] Haure-Mirande JV, Audrain M, Ehrlich ME, Gandy S. Microglial TYROBP/DAP12 in Alzheimer's disease: Transduction of physiological and pathological signals across TREM2. Molecular Neurodegeneration. 2022; 17: 55. https://doi.org/10.1186/s13024-022-00552-w.

[29] Turnbull IR, McDunn JE, Takai T, Townsend RR, Cobb JP, Colonna M. DAP12 (KARAP) amplifies inflammation and increases mortality from endotoxemia and septic peritonitis. The Journal of Experimental Medicine. 2005; 202: 363–369. https://doi.org/10.1084/jem.20050986.

[30] Pei J, Zhang J, Yu C, Luo J, Wen S, Hua Y, *et al*. Transcriptomics-based identification of TYROBP and TLR8 as novel macrophage-related biomarkers for the diagnosis of acute rejection after kidney transplantation. Biochemical and Biophysical Research Communications. 2024; 709: 149790. https://doi.org/10.1016/j.bbrc.2024.149790.

[31] Tammaro A, Stroo I, Rampanelli E, Blank F, Butter LM, Claessen N, *et al*. Role of TREM1-DAP12 in renal inflammation during obstructive nephropathy. PloS One. 2013; 8: e82498. https://doi.org/10.1371/journal.pone.0082498.

[32] Yamanishi Y, Kitaura J, Izawa K, Kaitani A, Komeno Y, Nakamura M, *et al*. TIM1 is an endogenous ligand for LMIR5/CD300b: LMIR5 deficiency ameliorates mouse kidney ischemia/reperfusion injury. The Journal of Experimental Medicine. 2010; 207: 1501–1511. https://doi.org/10.1084/jem.20090581.

[33] Ersahin T, Tuncbag N, Cetin-Atalay R. The PI3K/AKT/mTOR interactive pathway. Molecular BioSystems. 2015; 11: 1946–1954. https://doi.org/10.1039/c5mb00101c.

[34] Xiao H, Sun X, Lin Z, Yang Y, Zhang M, Xu Z, *et al*. Gentiopicroside targets PAQR3 to activate the PI3K/AKT signaling pathway and ameliorate disordered glucose and lipid metabolism. Acta Pharmaceutica Sinica. B. 2022; 12: 2887–2904. https://doi.org/10.1016/j.apsb.2021.12.023.

[35] Zhang B, Zeng M, Li B, Kan Y, Wang S, Cao B, *et al*. Arbutin attenuates LPS-induced acute kidney injury by inhibiting inflammation and apoptosis via the PI3K/Akt/Nrf2 pathway. Phytomedicine: International Journal of Phytotherapy and Phytopharmacology. 2021; 82: 153466. https://doi.org/10.1016/j.phymed.2021.153466.